

## THREE-DIMENSIONAL CHANGES IN LYMPHATIC ARCHITECTURE AROUND VX2 TONGUE CANCER — DYNAMICS OF GROWTH OF CANCER —

S. Seki, A. Fujimura

First Department of Oral and Maxillofacial Surgery (SS), First Department of Oral Anatomy (AF),  
School of Dentistry, Iwate Medical University, Morioka, Japan

### ABSTRACT

*Many questions remain regarding the mechanism of cervical lymph node metastasis via lymphatic vessels. We report here the three-dimensional dynamics of the lymphatic architecture around tumor during growth of implanted VX2 tongue cancer.*

*The tongue and the deep cervical lymph nodes of rabbits were observed at 3, 7 and 10 days after transplantation of VX2 cancer cells (n=5 in each group). Lymph node metastasis was confirmed histopathologically. Morphological changes of the collecting lymphatic vessels and lymphatic capillaries were observed, and the number and diameter of these lymphatic vessels were measured within 500  $\mu\text{m}$  around the tumor using the combined method of 5'-nucleotidase (5'-Nase) staining and three-dimensional reconstruction imaging.*

*The VX2 cells were uniformly detected in cervical lymph nodes of each rabbit of the 10-day group. The number of lymphatic capillaries and the diameters of collecting lymphatic vessels around the tumor in the 7- and 10-day groups were greater than in the 3-day group. These capillaries arose by sprouting from preexisting lymphatic vessels and showed a tree-like branching pattern.*

*We conclude that the dynamics of the lymphatic architecture around the tumor, especially the increase in number of capillaries on preexisting lymphatic vessels outside the*

*tumor margin, may be associated with lymph node metastasis.*

Metastasis to cervical lymph nodes is frequently found clinically, which adversely affects the prognosis for patients with oral squamous cell carcinomas (1,2). Anatomically, metastasis to the cervical lymph nodes is established by cancer cell invasion via the lymphatic vessels. Therefore, it is important to elucidate the mechanism of cervical lymph node metastasis to investigate changes in the microcirculation, especially of the lymphatics, during the development of cancer.

The 9,10-dimethyl 1,2-benzanthracene acetone-induced tongue carcinoma (3,4), VX2 transplanted tongue carcinoma (5) and human biopsy specimens of squamous cell carcinomas of the oral region (6-8) have been monitored for morphological changes of the lymphatics around tumor using 5'-nucleotidase (5'-Nase) staining. Furthermore, lymphangiogenesis within or around tumors has been reported in recent years, and the correlation between tumor lymphangiogenesis and regional lymph node metastasis has received increased attention (9,10). However, it is necessary for appreciation of the detailed morphological changes of lymphatics to observe the three-dimensional changes of lymphatic vessels around the tumor in the development of cancer. Fujimura et al have studied the three-dimensional lymphatic

architecture in the normal tongue of the rabbit using a method that combines 5'-Nase staining and three-dimensional reconstruction imaging (11).

In this study, we report the three-dimensional dynamics of the lymphatic architecture during the growth of VX2 tongue cancer in rabbits.

## MATERIALS AND METHODS

### *Animals and Tumor Cells*

Japanese white male rabbits (Oriental Bio Co., Ltd., Japan) (n=15), weighing 2.0-2.5 kg, were used in this study. They were maintained in a standard environment (room temperature:  $22 \pm 2^\circ\text{C}$ , room humidity:  $55 \pm 5\%$ ) in the vivarium of Iwate Medical University. The rabbits received a standard pellet diet with water ad libitum.

We used VX2 cells, which were transplantable into the rabbit tongue and readily spread to the regional lymph nodes (12,13). The VX2 cell line was maintained by successive transplantations at a position on the inside of the right leg muscle. Cancer cells were isolated from the leg muscle under sterile conditions, fragmented into fine pieces, filtered through a steel mesh, and suspended in saline. All experiments were carried out according to the guidelines of the Animal Experiment Committee of our Institute.

### *Animal Experiments*

Rabbits were injected with  $5 \times 10^5$  VX2 tumor cells in the left lateral border of the tongue under sodium pentobarbital anesthesia. They were killed by lethal injection of sodium pentobarbital at 3, 7 or 10 days after transplantation (n=5 in each group), and the tongue and both sides of the deep cervical lymph nodes of each rabbit were dissected. The primary tumors on the tongue were measured using a caliper, and the tumor volume was calculated according to the

formula  $a^2b/2$ , where  $a$  and  $b$  were the shortest and the longest diameter of the tumor, respectively.

The tongues were divided into two parts: An anterior part for histopathological examination by hematoxylin and eosin (H-E) staining and a posterior part for identification of the lymphatic vessels by 5'-Nase staining. The deep cervical lymph nodes were observed histopathologically for confirmation of metastasis by H-E staining.

### *Serial Cryosectioning and 5'-Nase Staining*

The specimens for 5'-Nase staining were immersed for 30 minutes in cold 4% formaldehyde-1% calcium chloride. After washing in 0.1M Tris-maleate buffer (pH 7.2), they were frozen in hexane ( $-80^\circ\text{C}$ ) cooled by dry ice. The frozen specimens were then embedded in 5% carboxymethyl cellulose (CMC) gel, and immediately frozen in the same hexane. The frozen specimen in the CMC block was cut using a cryostat (Bright Instrument. Co. Ltd., UK) and a cryofilm transfer kit (Finetec, Japan) devised by Kawamoto and Shimizu (14). We produced one hundred of the 10 ( $\mu\text{m}$ ) thick serial cryosections by these methods.

After washing with 0.1M Tris-maleate buffer, sections were incubated for 30 minutes at  $37^\circ\text{C}$  in the 5'-Nase substrate solution (15). The sections were washed in 0.1M Tris-maleate buffer, and incubated in 1% ammonium sulfide solution for 2 minutes. The sections were rinsed with distilled water and then mounted with glycerin.

### *Three-Dimensional Reconstruction of Lymphatic Vessels*

The three-dimensional reconstruction from serial sections of 5'-Nase staining was carried out according to the method devised by Fujimura et al (11,16). The sections were observed and input to a computer (Macintosh G4, Apple Co., USA) as two-dimensional image data using an optical microscope

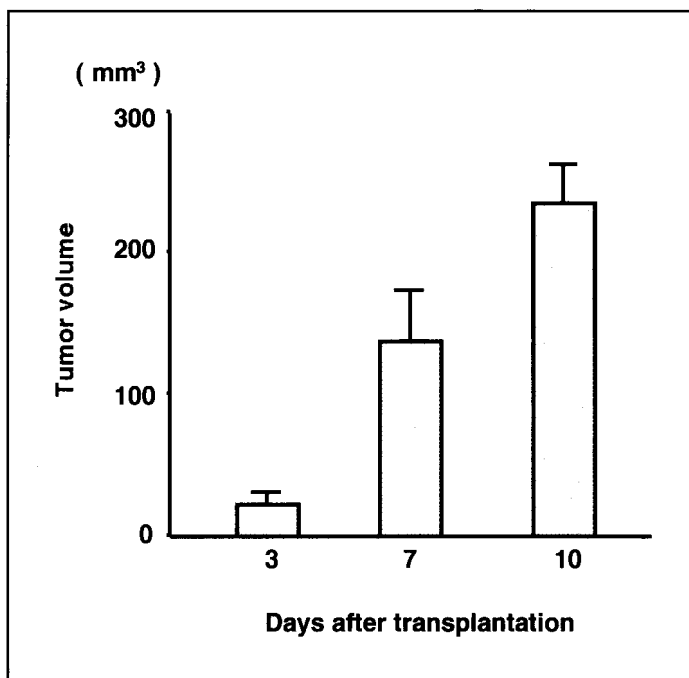


Fig. 1: Change in tumor volume of VX2 tongue cancer after transplantation. Data are presented as mean $\pm$ SD.

(E800, Nikon, Japan) equipped with a color chilled 3CCD video camera (C5810, Hamamatsu Photonics, Japan). The lymphatic vessels positive for 5'-Nase staining were extracted from these two-dimensional images, underwent threshold treatment in the computer (Photoshop ver. 7.0, Adobe Systems Inc., USA) and then were reconstructed to produce three-dimensional images by the volume-rendering method (VoxBlast ver. 2.3.3, VayTec, USA). A rotation image of the three-dimensional architecture of lymphatic vessels around the tumor was produced and observed from various perspectives.

#### *Number and Diameter of Lymphatic Vessels*

We have observed the superior longitudinal muscles accompanying collecting lymphatic vessels (SLCL), which are a major route for lymphatic vessels in the normal tongue of rabbits (11). In addition, there are vertical muscles, joined to the SLCL,

accompanying collecting lymphatic vessels (VL) (11). We observed morphological changes of the SLCL as well as in lymphatics joining the SLCL and in lymphatic capillaries, and measured the number and diameter of these lymphatic vessels within 500  $\mu$ m around the tumor. We counted the number of lymphatic capillaries using the rotation images. The largest diameter of the SLCL was confirmed on the three-dimensional image and then was measured on the two-dimensional image at this position.

For statistical evaluation of the data, we used the Mann-Whitney t-test, significance level of  $P < 0.05$  by InStat (ver. 2.03).

#### *RESULTS*

##### *Tumor Volume and Histopathological Findings of VX2 Tumor*

The mean volumes of the VX2 tumor of the 3-, 7- and 10-day groups were

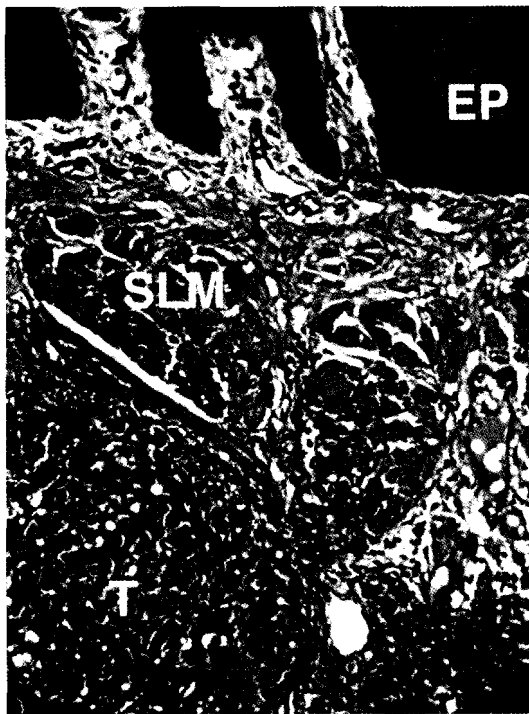


Fig. 2: Histological section of tongue at 7 days after transplantation. (H-E staining, X10). Infiltration of tumor cells and inflammatory cells. Ep: epithelium; SLM: superior longitudinal muscles; T: tumor cells.

$21.67 \pm 7.28$  (mm<sup>3</sup>),  $136.00 \pm 36.15$  (mm<sup>3</sup>), and  $233 \pm 28.24$  (mm<sup>3</sup>), respectively. The mean volume of primary tumors increased steadily from 3 days after transplantation (Fig. 1).

The tumor proliferated and infiltrated within the muscle of the transplanted side but not into the opposite side. In the 3-day group, tumor cells lodged in the muscle layer into which cells had been transplanted. In the 7-day group, tumor margin showed a cord-like invasion into muscle bundles. The tumor proliferated and infiltrated within vertical and transverse muscles but not into the upper longitudinal muscles or the submucosal lamina propria under the epithelium of the tongue. The area of the tumor was greater than in the 3-day group. In the tumor stroma, there were thick blood capillaries and chronic inflammatory cell infiltrates (Fig. 2). In the

muscle layer of the tumor periphery, muscles were slightly compressed by the growing tumor. In these muscles, there were dorsal branches of the deep lingual artery and veins that were compressed by muscles with growth of tumor. In the 10-day group, the area of tumor was greater than that in the 7-day group but there was no difference in findings around the tumor in the 7-day group.

#### *Lymph Node Metastasis of VX2 Tumor*

Although the hyperplasia of paracortical areas and the cellular reaction in the deep cervical lymph nodes were confirmed in the 3- and 7-day groups, lymph node metastasis of VX2 cells was not confirmed by histopathological examination. However, VX2 cells were observed in the deep cervical lymph nodes of all rabbits in the 10-day group (Fig. 3).

#### *Distribution and Three-Dimensional Architecture of Lymphatic Vessels Around Tumor*

5'-Nase-positive lymphatic vessels were not observed in the tumor area but instead in the musculature surrounding the tumor, where VX2 cells did not invade (Fig. 4). In the 3-day group, collecting lymphatic and lymphatic vessels existed in the muscle layer around the tumor (Fig. 5a,b). Specifically, there was SLCL in a border between the upper longitudinal muscle and the transverse muscle, and there were VL and lymphatic capillaries joined to the VL in the endomysium of the vertical muscle around the tumor (Fig. 5c,d). The mean of the numbers of lymphatic capillaries was  $8.2 \pm 1.0$ , and the mean of the diameters of the SLCL was  $75.0 \pm 12.9$   $\mu$ m.

In the 7-day group, the VL and SLCL within 50 to 100  $\mu$ m outside of the muscle bundles invaded by VX2 cells were pressed to the side of the septum, to the dorsum of the tongue more than in the 3-day group (Fig. 6a,b). There were a few lymphatic capillaries

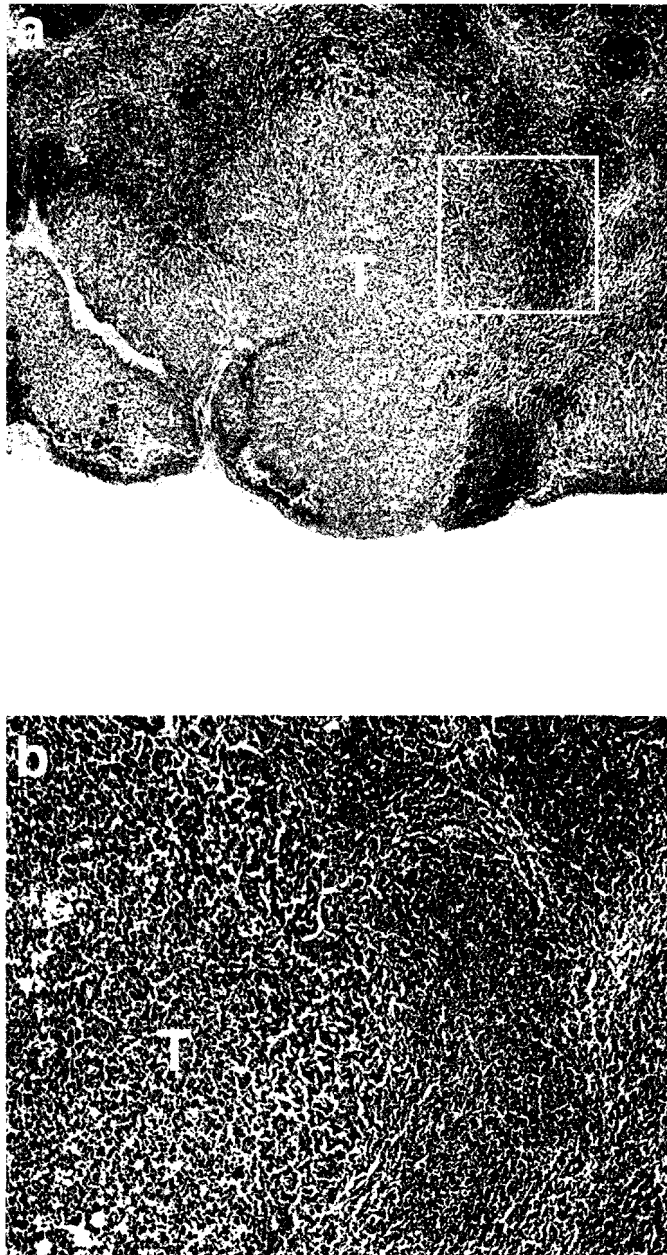


*Fig. 3: Histological section of the deep cervical lymph node at 10 days after transplantation. (H-E staining, a: X4, b: X10). T: tumor cells.*

less than 100  $\mu\text{m}$  from the tumor periphery. In the range of 100 to 300  $\mu\text{m}$  outside of the tumor periphery, lymphatic capillaries in the endomysium were observed on the VL and the location where the VL joined the SLCL

(*Fig. 6c,d*). The mean number of lymphatic capillaries was  $12.0 \pm 2.8$ , which was increased significantly more than in the 3-day group (*Fig. 7a*). The mean diameter of the SLCL was  $105.0 \pm 23.5 \mu\text{m}$ , which was

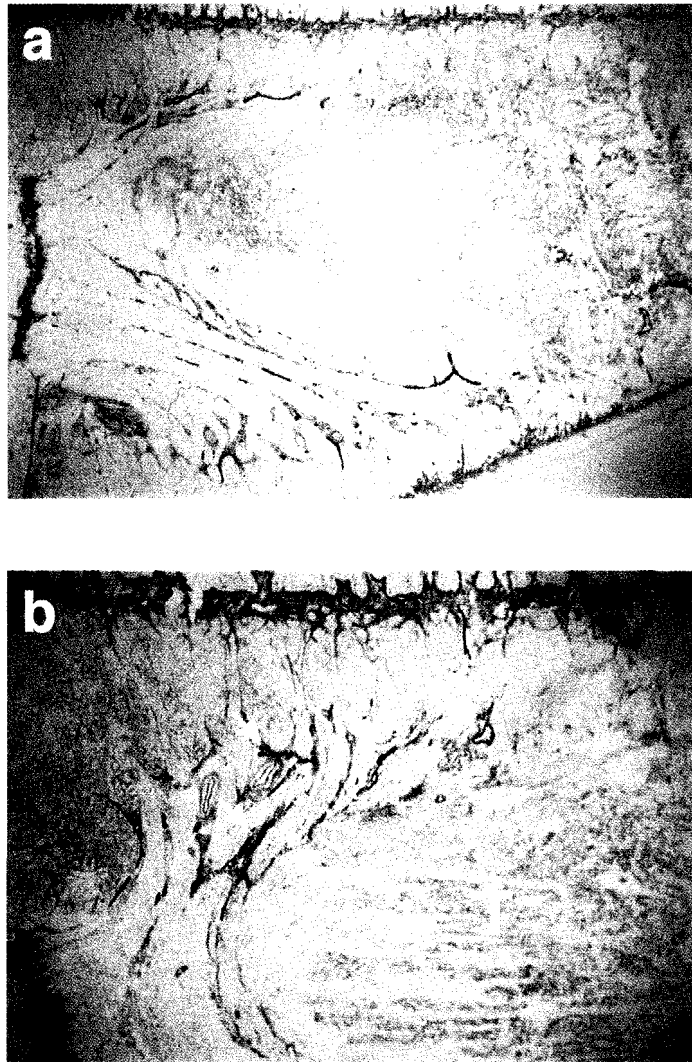


Fig. 4: Two-dimensional images of lymphatic vessels around tumor at 10 days after transplantation. (5'-Nase staining, a: X2, b: X4); arrow: SLCL; T: tumor.

significantly larger than in the 3-day group (Fig. 7b). The largest diameter was located where the VL joined the SLCL.

In the 10-day group, the VL and SLCL within 50 to 100  $\mu\text{m}$  outside of the muscle bundles invaded by VX2 cells were pressed intensely to the side of septum and to the dorsal side more than in the 7-day group, respectively. There were a few lymphatic capillaries closer than 100  $\mu\text{m}$  from the tumor periphery, as in the 7-day group. In the range

of 100 to 300  $\mu\text{m}$  outside of the tumor periphery, lymphatic capillaries, about 30 to 50  $\mu\text{m}$  long, were seen on the VL (Fig. 8a,b). The mean number of these capillaries was  $16.0 \pm 2.8$ , which was increased significantly more than in the 3-day group (Fig. 7a). These capillaries had no consistent pattern of branching and showed a tree-like branching pattern rather than a network pattern (Fig. 8c,d). The mean diameter of the SLCL was  $118.0 \pm 15.3 \mu\text{m}$ , which was significantly

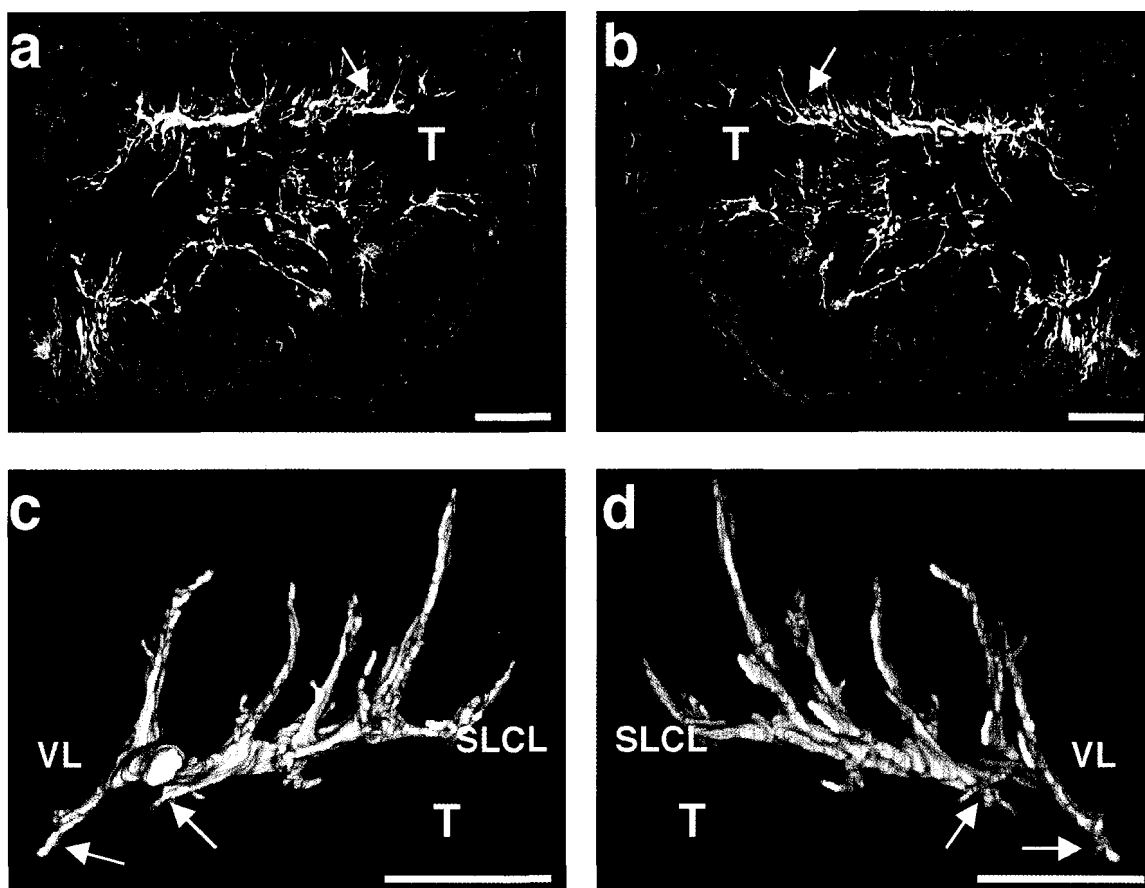


Fig. 5: Three-dimensional lymphatic architecture around tumor at 3 days after transplantation. (a, b: X2, c, d: X4). Lymphatic capillary (arrow); T: tumor; Bar: 500  $\mu$ m.

larger than in the 3-day group (Fig. 7b). The part of the SLCL that VL joined had the largest diameter, as in the 7-day group. There were no significance differences between the mean numbers and diameters of the 10-day group compared with the 7-day group.

#### DISCUSSION

This report presents a three-dimensional image of lymphatic architecture around the tumor during growth of VX2 tongue cancer in rabbits.

The SLCL evaluated in this study is one of the main routes of lymphatic vessels in the normal tongue of the rabbit (11). The SLCL

runs in the front and back direction between the superior longitudinal muscle and the transverse muscle and forms a ladder-like network (11). VX2 tongue cancer infiltrates these muscles and destroys lymphatic vessels within them. In this study, we observed morphological changes of lymphatic vessels around the tumor. The number of lymphatic capillaries around the tumor in 7- and 10-day groups increased more than in 3-day group. Lymphatic capillaries arose by sprouting from preexisting lymphatic vessels, the VL, on the normal muscle bundles within 100-300  $\mu$ m outside of the tumor periphery. These capillaries showed a tree-like branching pattern.

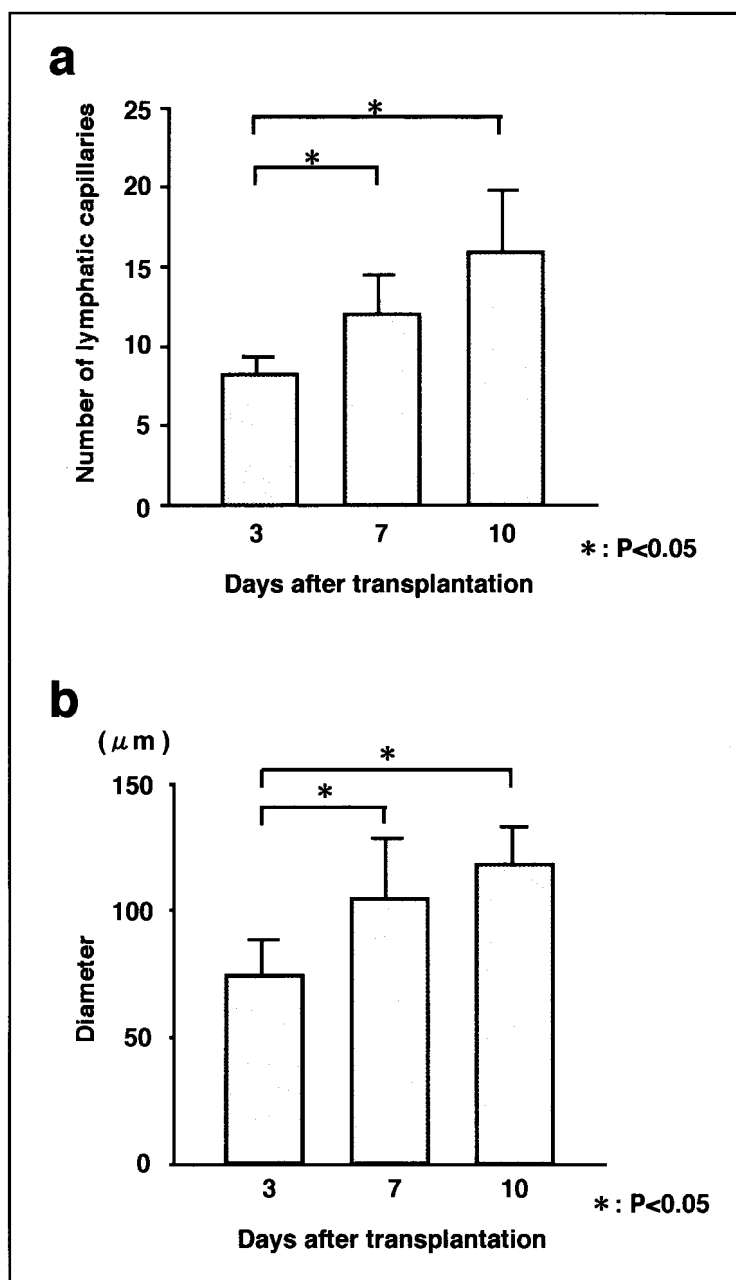


Fig. 7: Number of lymphatic capillaries and diameter of ULCL. a: Number of lymphatic capillaries; b: diameter of ULCL (mean±SD).

newly formed from preexisting lymphatic vessels in normal tissue outside the tumor margin before cancer cell invasion. Furthermore, it appears that the LCL, VL,

and lymphatic capillaries are routes of metastasis to the cervical lymph nodes.

The distribution and architecture of lymphatic capillaries in the normal tongue of



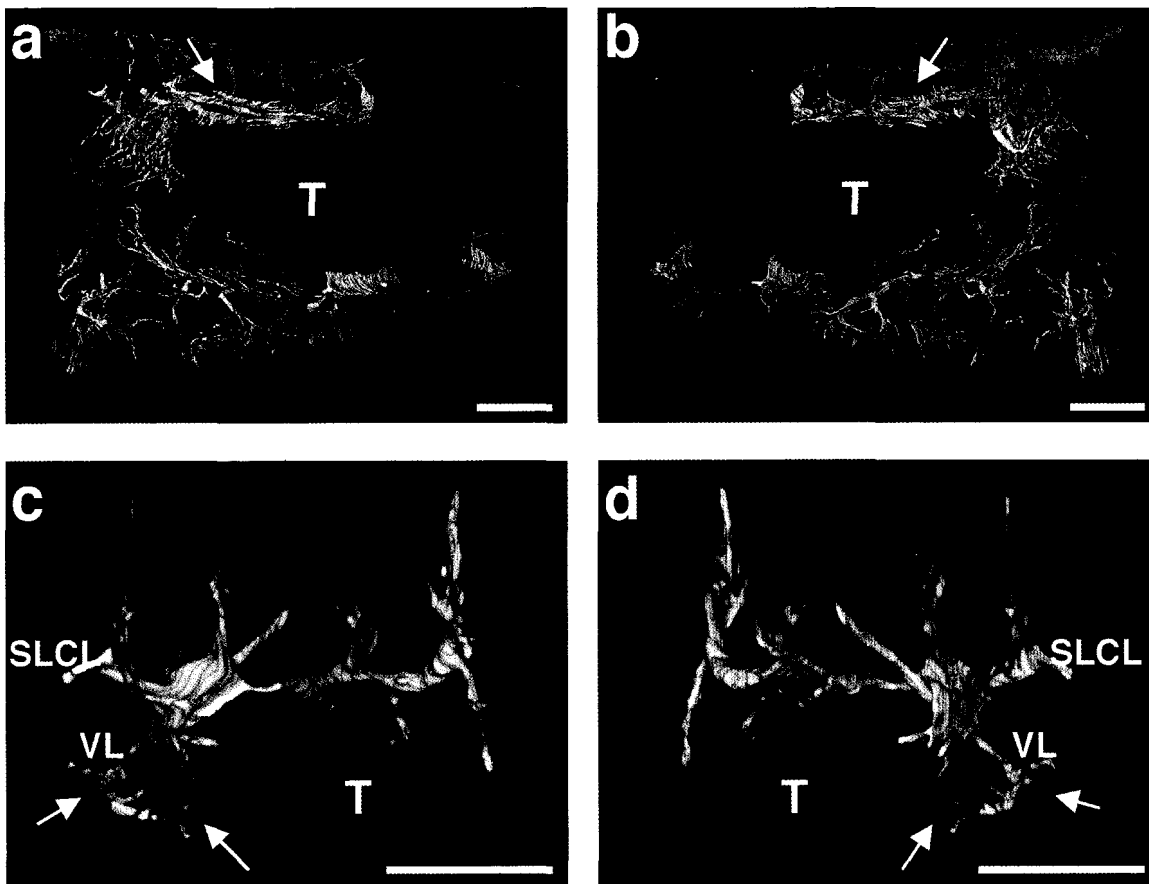


Fig. 8: The three-dimensional lymphatic architecture around tumor at 10 days after transplantation. (a, b: X2, c, d: X4). Lymphatic capillary (arrow); T: tumor; Bar: 500  $\mu$ m.

the golden hamster are morphologically different between the dorsal and the sublingual side of the lamina propria (25). Blind end lymphatic capillaries, which arise from the lymphatic capillary network in the lamina propria enter into the papilla of the lamina propria. In contrast, lymphatic capillaries in the sublingual surface form a hexagonal network, with no blind end lymphatic capillaries arising from this network. These results suggest that the lymphatic architecture depends on the peripheral structure (25). On the other hand, VX2 cancer cells infiltrate in a cord-like fashion the peripheral normal tissue, and the margin of the tumor is irregular. However,

the blind ends of lymphatic capillaries neither enter the irregular margin of the tumor nor form the lymphatic capillary network around the tumor. There is little distribution of lymphatic vessels closer than 100  $\mu$ m around the tumor. In addition, blood vessels form a network around the tumor, but lymphatic vessels do not. We hypothesize that lymphatic vessels have particular characteristics in pathological conditions but are not affiliates of blood vessels.

Lymphatic vessels have a functional role in maintaining homeostasis of the interstitial fluid (26). Some authors report enlarged lymphatic capillaries during the growth of cancer cells in 9,10-dimethyl 1,2-

benzanthracene acetone-induced tongue carcinoma (4), VX2 transplanted tongue cancer (5), and human biopsy specimens of squamous cell carcinomas of the oral region (8). Ogawa has reported that the transport of substances especially via intracellular endothelial spaces and pinocytotic vesicles increases with progression of tumor in lymphatic capillaries surrounding the tumor (27). The mean diameters of the SLCL in the 7- and 10-day groups are significantly larger than in the 3-day group. The largest diameter of the SLCL is located where the VL joins the SLCL. These findings suggest that the diameters of collecting lymphatics are enlarged by increased lymph flow.

Metastasis to the deep cervical lymph nodes in the VX2 tongue cancer model began during 7 and 14 days after transplantation (28). In this study, lymph node metastasis was confirmed in the 10-day group. At that time, the number of lymphatic capillaries around the tumor was increased. These results suggest that an increased number of lymphatic capillaries increases the likelihood of cancer cell invasion into the lymphatics.

In conclusion, our results suggest that the dynamics of the lymphatic architecture around the tumor, especially the increased number of capillaries from preexisting lymphatic vessels outside of the tumor margin, is associated with lymph node metastasis. Interestingly, He et al have recently reported that inhibition of the VEGFR-3 signaling can block tumor lymphangiogenesis and suppress lymph node metastasis (29). Further studies are required to clarify the dynamics of the lymphatic architecture around the tumor by administering anticancer agents.

#### ACKNOWLEDGMENT

We are especially thankful for the advice and expertise of Prof. Yohichiro Nozaka. We also wish to thank Prof. Harumi Mizuki and Prof. Masanobu Satoh for advising and reading the manuscript. In addition, we would like to thank Dr. Keigo Kudo,

Dr. Atsushi Ogawa, Dr. Masao Onodera and the staff at our departments for advising us about experimental methods in this study. We thank Amato Pharmaceutical Products, Ltd., Japan for kindly accepting the joint study. This work was supported by a scientific research grant from the Japanese Ministry of Education (No. 13671908, 14571741), the Promotion and Mutual Aid Corporation for Private Schools of Japan, and the High Tech Research Subsidy of a Scientific Study of the Japanese Ministry of Education.

#### REFERENCES

1. Honma, Y: A study on metastasis to the cervical lymph node of oral cancer. *Jpn. J. Oral Maxillofac. Surg.* 28 (1982), 1667-1684.
2. Tateda, M, K Shiga, S Saijo, et al: A clinical study of oral tongue cancer. *Tohoku J. Exp. Med.* 192 (2000), 49-59.
3. Endo, M: An experimental study on the distribution and structure of lymphatic capillaries in the connective tissue underlying induced tongue cancer. *Dent. J. Iwate Med. Univ.* 18 (1993), 36-50.
4. Nakayama, A: Enzyme-histochemical observation of lymphatic capillaries in induced tongue cancer. *Jpn. J. Oral Maxillofac. Surg.* 41 (1995), 104-113.
5. Kitahara, T: Observation of lymphatic vessels using 5'-Nase staining method in the VX2 tongue cancer. *Dent. J. Iwate Med. Univ.* 20 (1995), 270-283.
6. Endo, M, A Nakayama, Y Fukuta, et al: Enzyme-histochemical staining method for lymphatic capillaries of oral carcinomas. *Head and Neck Cancer* 20 (1994), 44-49.
7. Ogawa, A, A Nakayama, M Endo, et al: Enzyme-histochemical observation of lymphatic vessels in the stroma of oral squamous cell carcinoma *Jpn. J. Oral Maxillofac. Surg.* 42 (1996), 25-29.
8. Nakayama, A, A Ogawa, Y Fukuta et al: Relation between lymphatic vessel diameter and clinicopathologic parameters in squamous cell carcinomas of oral region. *Cancer* 86 (2000), 200-206.
9. Beasley, JPN, R Prevo, S Banerji, et al: Intratumoral lymphangiogenesis and lymph node metastasis in head and neck cancer. *Cancer Res.* 62 (2002), 1315-1320.
10. Mattila, MM-T, JK Ruohola, T Karpanen, et al: VEGF-C induced lymphangiogenesis is

- associated with lymph node metastasis in orthotopic MCF7 tumors. *Int. J. Cancer* 98 (2002), 946-951.
11. Fujimura, A, S Seki, M-Y Leo, et al: Three-dimensional architecture of lymphatic vessels in tongue. *Lymphology* 36 (2003), 120-127.
  12. Jefferis, AF, MC Berenbaum: The rabbit VX2 tumour as a model for carcinomas of the tongue and larynx. *Acta Otolaryngol.* (Stockh.) 108 (1989), 152-160.
  13. Toyama, K: A histopathological study on carcinoma of the tongue produced by Vx2 carcinoma. *J. Kyushu Dent. Soc.* 32 (1978), 340-356.
  14. Kawamoto, T, M Shimizu: A method for preparing 2- to 50- $\mu$ m-thick fresh-frozen sections of large samples and undecalcified hard tissues. *Histochem. Cell Biol.* 113 (2000), 331-339.
  15. Kato, S: Histochemical localization of 5'-nucleotidase in the lymphatic endothelium. *Acta Histochem. Cytochem.* 23 (1990), 613-620.
  16. Fujimura, A, Y Nozaka: Analysis of the three-dimensional lymphatic architecture of the periodontal tissue using a new 3D reconstruction method. *Microsc. Res. Techniq.* 56 (2002), 60-65.
  17. Pepper, MS: Lymphangiogenesis and tumor metastasis: Myth or reality? *Clin. Cancer Res.* 7 (2001), 462-468.
  18. Clarijs, R, DJ Ruiter, RMW de Waal: Lymphangiogenesis in malignant tumours: Does it occur? *J. Pathol.* 193 (2001), 143-146.
  19. Jain, RK, BT Fenton: Intratumoral lymphangiogenesis: A case of mistaken identity or malfunction? *J. Nat. Cancer Inst.* 94 (2002), 417-421.
  20. Leu, AJ, DA Berk, A Lymboussaki, et al: Absence of functional lymphatics within a murine sarcoma: A molecular and functional evaluation. *Cancer Res.* 60 (2000), 4324-4327.
  21. Pullinger, BD, HW Florey: Proliferation of lymphatics in inflammation. *J. Pathol. Bacteriol.* 45 (1937), 157-170.
  22. Clark, ER, LC Clark: Observations on the new growth of lymphatic vessels as seen in transparent chambers introduced into the rabbit ear. *Am. J. Anat.* 51 (1932), 49-87.
  23. Paavonen, K, P Puolakkainen, L Jussila, et al: Vascular endothelial growth factor receptor-3 in lymphangiogenesis in wound healing. *Am. J. Pathol.* 156 (2000), 1499-1504.
  24. Takeda, N: Three-dimensional analysis of tumor vessels in transplanted VX2 tongue cancer. *Dent. J. Iwate Med. Univ.* 22 (1997), 228-241.
  25. Liang, J-C, A Fujimura: Lymphatic architecture beneath the mucosal membrane of the tongue. *Dent. J. Iwate Med. Univ.* 25 (2000), 283-291.
  26. Leak, LV, VJ Ferrans: Lymphatics and lymphoid tissue. In: *The Lung, Scientific Foundations*. Crystal, RO, JB West (Eds.), 1st Ed, Raven Press Ltd, New York (1991), p779-786.
  27. Ogawa, A: HRP absorption on endothelial cell of the lymphatic capillary in the rabbit VX2 tongue carcinoma. *Dent. J. Iwate Med. Univ.* 21 (1996), 242-256.
  28. Matsuura, M: Metastasis and cellular of the cervical lymph nodes in a rabbit VX2 tongue cancer model. *Jpn. J. Oral Maxillofac. Surg.* 42 (1996), 29-41.
  29. He, Y, K Kozaki, T Karpanen, et al: Suppression of tumor lymphangiogenesis and lymph node metastasis by blocking vascular endothelial growth factor receptor 3 signaling. *J. Nat. Cancer Inst.* 94 (2002), 819-825.

**Shotaro Seki, DDS**

**First Department of Oral and  
Maxillofacial Surgery**

**(Chief Professor: Harumi Mizuki)**

**School of Dentistry**

**Iwate Medical University**

**1-3-27 Chuo-dori, Morioka 020-8505, Japan**

**Phone: +81-19-621-3661**

**Fax: +81-19-621-3662**

**E-mail: akifuji@iwate-med.ac.jp**